GPS Based Attitude Determination
The REX II Flight Experience

Douglas Freesland[*], Keith Reiss[†], David Young[‡] and Jon Cooper[§]
CTA Space Systems
1521 Westbranch Dr · McLean, VA 22102

Captain Andrew Adams[**]
USAF Space Test Program
160 Skynet St · Los Angeles, CA 90245

Abstract

A milestone in the annals of satellite guidance, navigation and control was achieved as REX II became the first spacecraft to employ GPS attitude knowledge for closed-loop control. Successfully launched and activated on March 8, 1996, this highly capable, low cost, 242 lb spacecraft, uses a GPS receiver to provide the attitude knowledge required by the control system to maintain a three-axis nadir pointed orientation. This paper describes the spacecraft, its attitude control subsystem and by evaluating its early flight history, captures our on-orbit experience using GPS. The resulting combination of GPS attitude knowledge coupled with our simple yet elegant controller has allowed REX II to exceed mission requirements via highly autonomous modes of operations.

I. Spacecraft Overview

REX II was designed and constructed for the Air Force Space Test Program (STP) by CTA Space Systems (CTASS) in McLean, Virginia. Its mission is to operate two experimental payloads: a Rome Laboratory communications experiment, and a GPS attitude determination and control technology demonstration. The primary communications experiment advances research on electron density irregularities that cause disruptive scintillation effects on transionospheric radio signals. The secondary experiment demonstrates the first ever use of GPS attitude knowledge for closed-loop control.

The REX II spacecraft is illustrated in Fig. 1. Its design is based on two previous STP missions: the original REX spacecraft launched in June 91 and RADCAL launched in June 93. Technical characteristics are summarized in Table I. It was launched into a 450 nmi circular polar orbit aboard a Pegasus XL out of Vandenberg AFB on March 8, 1996.

Table I. Spacecraft Description

Structure
· 8 sided, 30″ diameter, 22″ tall
· Weight : 242 lbs
Attitude Control
· Three-axis nadir pointed

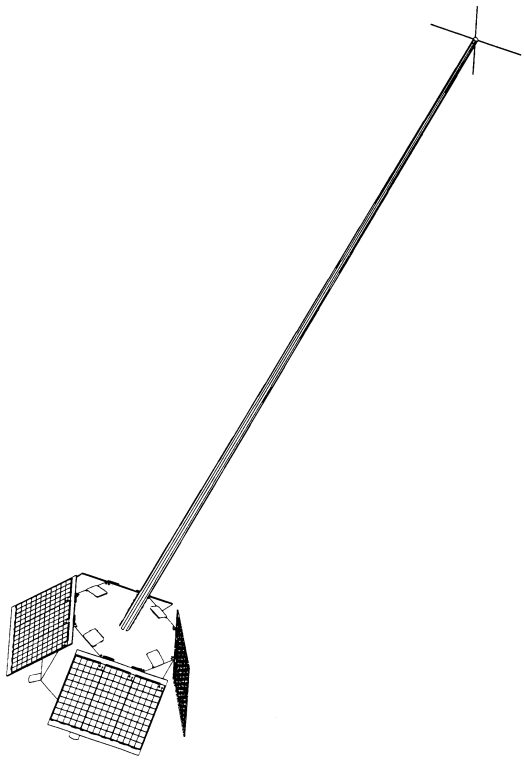

Fig. 1. The REX II spacecraft.

[*] Manager Attitude Determination and Controls
[†] Manager Software, Analysis/Mission Operations Group
[‡] REX II GPS Subsystem and Software Engineer
[§] REX II Program Manager (CTASS)
[**] REX II Project Manager (STP)

· Pitch momentum bias · Backup passive gravity gradient stabilized · GPS attitude determination
Power · 3 NiCd batteries · 4 deployed solar arrays · Orbit average power : 30 watts
TT&C · 2.4 kbps, 60 watt UHF uplink · 2.5 kbps, 18 watt UHF downlink · Blades and ring antenna · Backdoor spacecraft receiver
Thermal · Passive thermal control · Battery heaters
Mass Properties : deployed · Ixx : 71.2 ftlbsec^2 · Iyy : 71.2 ftlbsec^2 · Izz : 5.6 ftlbsec^2

For the first 40 days of the mission REX II was controlled out of the CTASS multi-mission satellite control facility in McLean. Following its successful activation and on-orbit checkout, routine operations were transferred to the Air Force.

II. Attitude Control Subsystem

The REX II mission requires three-axis nadir pointing with the spacecraft Z-axis pointed down along the local vertical and the negative Y-axis in the direction of the orbit normal. The X-axis completes the right handed coordinate system pointing in the direction of the orbital velocity as shown in Fig. 2. Specific ACS requirements include:

- Acquire nadir pointed orientation from any arbitrary attitude with rates at separation in the range 6 ± 3°/sec.
- Maintain nadir pointing to within ± 5°.

A pitch bias momentum system satisfies these requirements, selected for its minimum number of components, simplified flight software and ease of operations. The ACS functional block diagram is illustrated in Fig. 3 and includes both active and passive components.

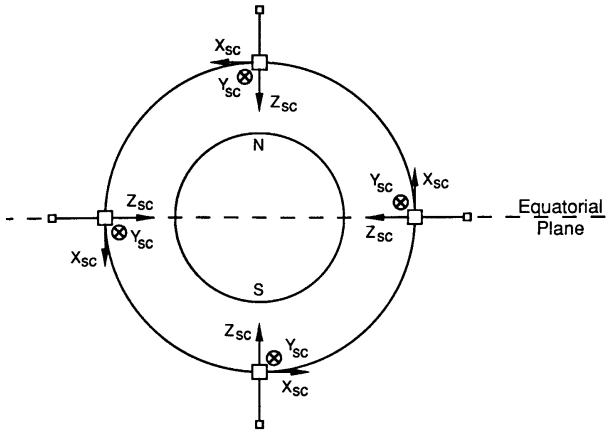

Fig. 2. Three-axis nadir pointed orientation.

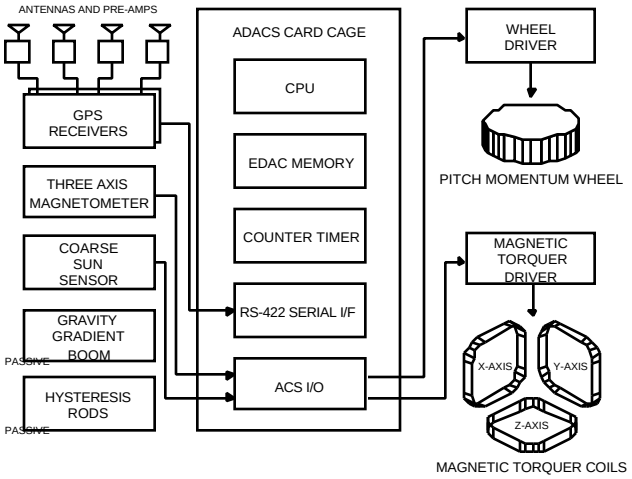

Fig. 3. ACS functional block diagram.

Hardware

ACS components are summarized in Table II. Three-axis attitude knowledge is provided by redundant Trimble Advanced Navigation Sensor (TANS) Vector receivers. Similar to the TANS Quadrex flown on RADCAL, a multiplexed front end allows the receiver to measure the differential carrier phase between the master and each of three slave antennas.[1] On RADCAL the receiver output the raw differential phase measurements which were processed on the ground to determine an attitude solution.[2,3] A second processor was added to the receiver on REX II to compute a real-time attitude solution on-board. Its firmware implements an attitude point solution algorithm which performs an iterative least squares fit to a set of simultaneous observations. The firmware is configured to output traditional roll, pitch and yaw angles describing the transformation from orbital to spacecraft frames using a 3-2-1 sequence of rotations. The receiver outputs these angles at a 1 Hz rate for use in the spacecraft processor where they are accumulated and averaged over the 5 sec ACS control cycle.

Table II. ACS Component Summary

Component	Vendor	Performance	
GPS Receiver & Antennas	Trimble	Position Velocity Attitude	100 m 0.2 m/sec 0.3° 1 m baseline
TAM	NanoTesla CTASS	Sensitivity Noise	0.5 Vdc/60000 nT < 2 nT rms
CSS	SPC	Field of view Accuracy	4πsteradian ~5°
Wheel	CTASS	Torque Momentum	0.018 ftlb 2.4 ftlbsec
Torquers	CTASS	2.6 Am^2 at 5 vdc	
GG Boom	CTASS	21 ft length, 4 lb tip mass	

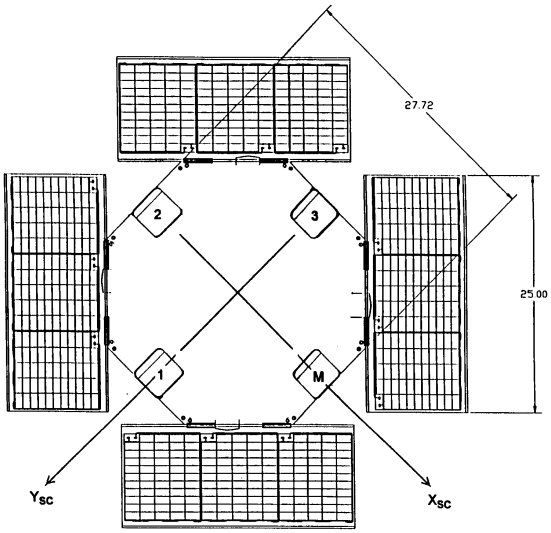

Fig. 4. Top plate GPS antenna mounting.

The configuration of the four GPS patch antennas is shown in Fig. 4. On RADCAL the antennas were canted away from zenith by 17.5° to reduce multipath reflections from its gravity gradient boom. On REX II the antennas are mounted flat, coplanar with the spacecraft top plate with each antenna keyed in the same direction to minimize errors associated with antenna patterns. The corresponding M-1, M-2 and M-3 baseline lengths are 42, 60 and 42 cm respectively. Mounting is controlled to assure < 0.1° misalignment between the antenna baselines and the spacecraft axes. Unlike RADCAL which used a roving master antenna selected based on the highest signal to noise ratio, REX II employs a fixed master.

Other sensors include the CTASS three-axis magnetometer (TAM) and coarse sun sensor (CSS). The TAM generates measurements of the local magnetic field for use on-board. The CSS consists of 12 individual solar angle detectors oriented to provide 4π steradian coverage. The signals are processed on-board to form the sun azimuth and elevation angles which are inserted into telemetry with the TAM data for use on the ground.

Bias momentum is provided by the CTASS wheel mounted with its spin axis aligned to within 0.1° of the spacecraft pitch axis. To develop the required -0.5 ftlbsec bias momentum, the wheel is operated at a constant speed of -955 rpm. Actuation is provided by CTASS air core magnetic torquers mounted in each axis. In the X and Y axes, space restrictions required that two smaller coils be wired in parallel for a total dipole of 2.6 am^2. A single coil provides the same 2.6 am^2 dipole in the Z-axis. To correct an inverted orientation, the Z-coil can be commanded to a higher operating voltage producing a maximum dipole of 85 am^2.

A hold over from earlier spacecraft in this series, passive stabilization is provided by a 21′ gravity gradient boom. Damping is provided by two 0.156″ diameter 20″ long nickel/iron magnetic hysteresis rods mounted at the tip of the boom.

Modes of Operation

Four modes are provided to support all phases of the mission. The acquisition sequence begins at launch vehicle separation and is completed with the spacecraft configured in its normal earth pointed orientation, pitch bias momentum wheel at nominal speed, gravity gradient boom and solar arrays deployed.

Separation

The spacecraft separates from the launch vehicle at any arbitrary attitude spinning at 6 ± 3°/sec about the spacecraft Z-axis as shown in Fig. 5.

Mode 1 : Initial Acquisition

Upon detection of separation the ACS is automatically activated in Mode 1. In this mode the TAM data and magnetic torquers are used in a Bdot control law to reduce magnetic rates to < 0.0015 gauss/sec in all three axes (Fig. 6). After the magnetic rates have been below the threshold for 5 consecutive

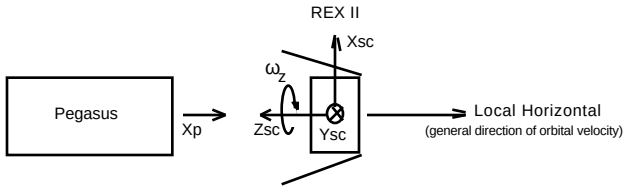

Fig. 5. Spacecraft orientation at separation.

ACS cycles, an autonomous switch to Mode 2 is made.

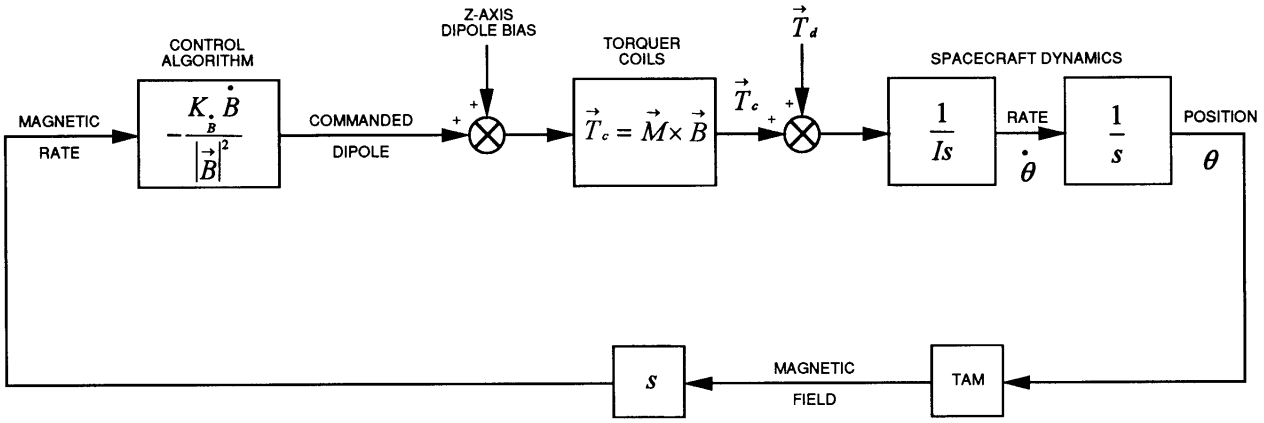

Fig. 6. Modes 1, 2 and 3 Bdot controller block diagram.

Mode 2 : Roll/Yaw Acquisition

Upon entrance to Mode 2 the pitch axis momentum wheel is turned on and driven to -955 rpm (-0.5 ftlbsec). This results in alignment of the spacecraft negative Y-axis with the orbit normal, rotating at twice orbital rate. The TAM data and magnetic torquers are used in the same Bdot control law as in Mode 1 with the exception that a 0.5 am^2 bias is added to the Z-axis dipole command. This forces the pitch rotation to be phased such that the spacecraft Z-axis is pointed down the local vertical over the north pole. The spacecraft continues to operate in this mode until commanded to Mode 3 from the ground.

Mode 3 : Pitch Acquisition/Safehold

The spacecraft is commanded to Mode 3 over the north pole when the Z-axis is pointed down along the local vertical. This is the ideal orientation for gravity gradient boom deployment. As in the previous modes a Bdot control law is used but with unique gains and no Z-axis dipole bias. The spacecraft acquires the desired nadir pointing attitude and continues to operate in this mode until commanded from the ground.

Mode 4 : Normal Mode

The spacecraft is commanded to Mode 4 after GPS attitude determination performance is verified. In this mode the GPS attitude solution is processed to provide three-axis attitudes and rates used in a cross product control law to generate the desired magnetic torquer drives (Fig. 7). In the roll and yaw axes, control is limited to latitudes within ± 45° of the equator where the magnetic field direction is optimal. This is the nominal mode of operation for the remainder of the mission.

To provide protection from operating in Mode 4 with erroneous attitude data, an autonomous switch to Mode 3 is made whenever the attitude solution is not valid for a consecutive number of ACS cycles. This is implemented by checking that: 1) GPS status bits indicate a valid solution, and 2) roll, pitch and yaw attitude errors are within ± 15°. Additional logic provides a switch back to the normal mode once the attitude solution has returned to a valid state for the required number of ACS cycles.

ACS simulation results are presented in Fig. 8 and illustrates a typical activation sequence from separation through normal mode transition. At separation the spacecraft is spinning at 6°/sec. After 2.6 hours the rates have been reduced and the wheel is automatically enabled followed by a switch to mode 3 and boom deployment 12.2 hours into the run. Finally, the transition to normal mode is commanded 24 hours after separation.

An error budget was established to quantify performance and is presented in Table III. The predicted steady state performance in Mode 3 is 3.1° while normal mode performance improves to 1.9°.

III. GPS Flight Data Performance Evaluation

Due to the slow 2.4 kbps downlink rate, ACS telemetry is typically collected for only one or two orbits per day. GPS performance evaluation required that long duration telemetry collects be scheduled. Of interest are the two telemetry collections listed in Table IV. The first covers the initial transition to normal mode using GPS attitude knowledge for closed-loop control. The second represents long term normal mode performance using GPS. The ACS telemetry in both data sets was collected at the rate of one sample every 6 minutes.

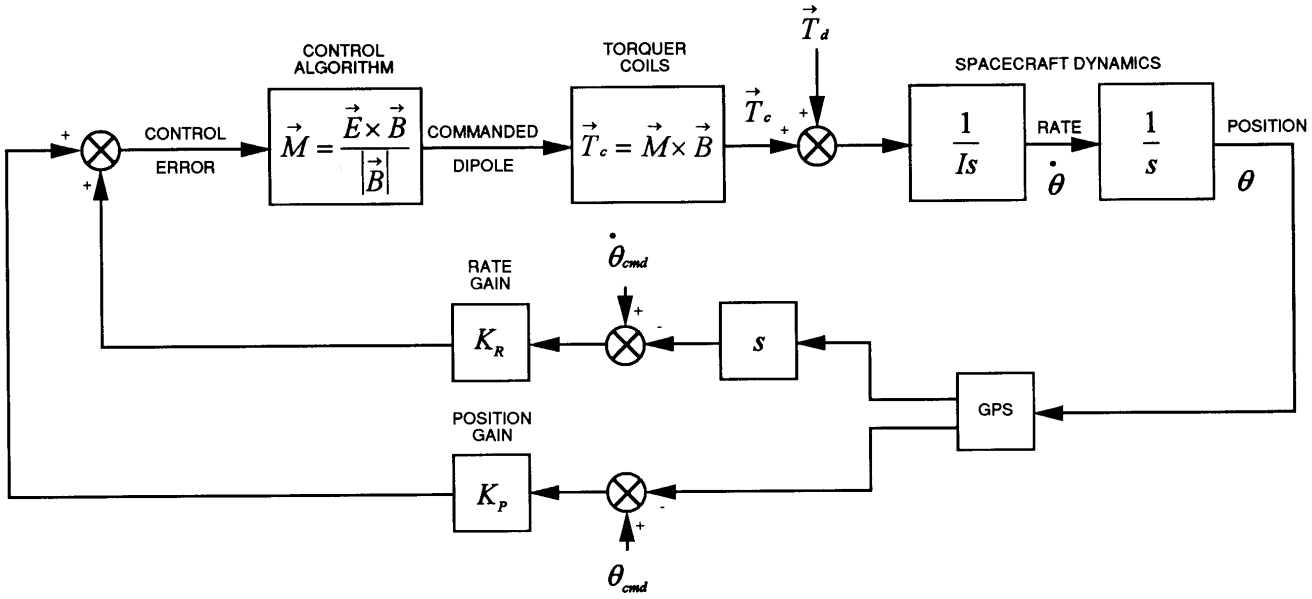

Fig. 7. Mode 4 normal mode controller block diagram.

Table III. Pointing Error Budget

Error Source	Mode 3	Mode 4
Attitude Knowledge		
Static RSS		0.10°
GPS Alignment		0.10°
Slow Dynamic RSS		0.01°
Thermal Distortion		0.01°
Fast Dynamic RSS		0.90°
GPS Accuracy		0.90°
Attitude Knowledge Sum		1.01°
Attitude Control		
Static RSS	0.51°	0.51°
TAM Alignment	0.50°	0.50°
Wheel Alignment	0.10°	0.10°
Slow Dynamic RSS	2.50°	1.00°
Controller Performance	2.50°	1.00°
Fast Dynamic RSS	0.11°	0.11°
TAM Accuracy	0.10°	0.10°
Wheel	0.03°	0.03°
Magnetic torquer	0.03°	0.03°
Attitude Control Sum	3.12°	1.62°
RSS Overall Accuracy	3.12°	1.91°
Requirement	5.00°	5.00°
Margin	1.88°	3.09°

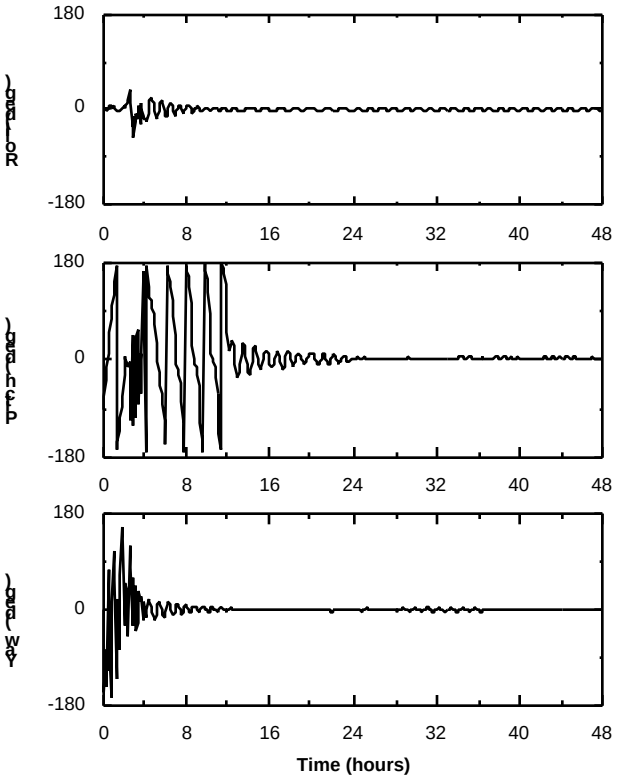

Fig. 8. Initial acquisition ACS simulation results.

Table IV. GPS Long Term Telemetry Collections

Data Set	Start Time	Stop Time	GPS Receiver
1	089:20:24:19	090:08:24:18	TANS-A
2	102:11:23:58	103:23:11:58	TANS-B

GPS Attitude Solution

The first switch to normal mode and use of GPS attitude knowledge for closed-loop control occurred on March 29, 1996. Roll, pitch and yaw attitudes as reported to the controller by the GPS TANS-A receiver are shown in Fig. 9. The transition from Mode 3 to Mode 4 is clearly visible. In Mode 3, interaction of the active Bdot controller with the passive gravity gradient stabilization, results in an expected pitch offset of -1.8°. Following the switch to normal mode, the offset is eliminated.

Long term performance in the normal mode is represented by the data illustrated in Fig. 10, collected over 36 hours starting on April 11, 1996. The figure shows roll, pitch and yaw attitudes as reported by GPS TANS-B. A dropout in the GPS attitude solution resulted in an autonomous transition to Mode 3, 28 hours into the data, followed by an autonomous return to Mode 4 once the GPS attitude solution was reacquired. Neglecting this transient, normal mode performance is summarized in Table V and is well within the 5° requirement. The mean attitude errors are most likely dominated by misalignments between the spacecraft axes and the principal axes which can easily occur if the boom is not deployed exactly along the negative Z axis.

Table V. Normal Mode Performance

	Roll	Pitch	Yaw
Max	3.09°	2.52°	5.16°
Min	-4.47°	-3.38°	-5.44°
Mean	-0.91°	-0.35°	0.21°
Sigma	1.65°	0.94°	1.96°

The peak-to-peak variations in roll and yaw, exceed that predicted by simulation. Fig. 11 illustrates the solar beta angle and sun light fraction for the REX II orbit. On April 11 the umbra duration was 29 minutes. A second trace was added to the graph of GPS yaw attitude in Fig. 10 to indicate when the spacecraft was in umbra. The data suggests a correlation between umbra and peak roll/yaw errors. The errors may result from thermal distortion of the GG boom at umbra transitions. Differential heating across the boom causes it to bend. Introduction of a thermal snap model into the ACS simulation with a maximum torque of -0.015 ftlb, 10 sec rise time and 80 sec decay time, results in the performance shown in Fig. 12, similar to that observed on orbit.

Long term nadir pointing performance is summarized in Fig. 13-14. A nadir pointing angle was constructed from the roll and pitch attitude reported by GPS using the April 11 data set. From this data a histogram was generated as shown in Fig. 13. A distribution of pitch vs roll attitude is presented in Fig. 14.

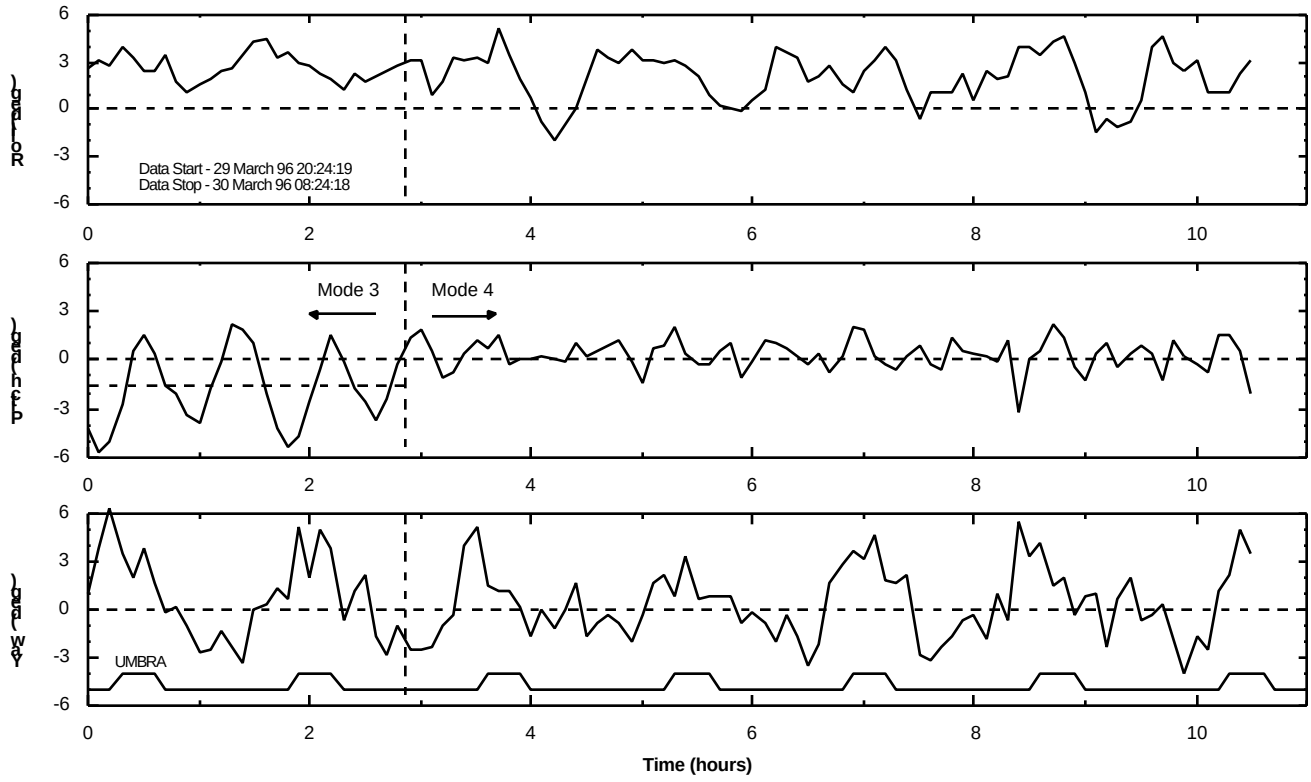

Fig. 9. GPS TANS-A attitude solutions : First transition to normal mode control.

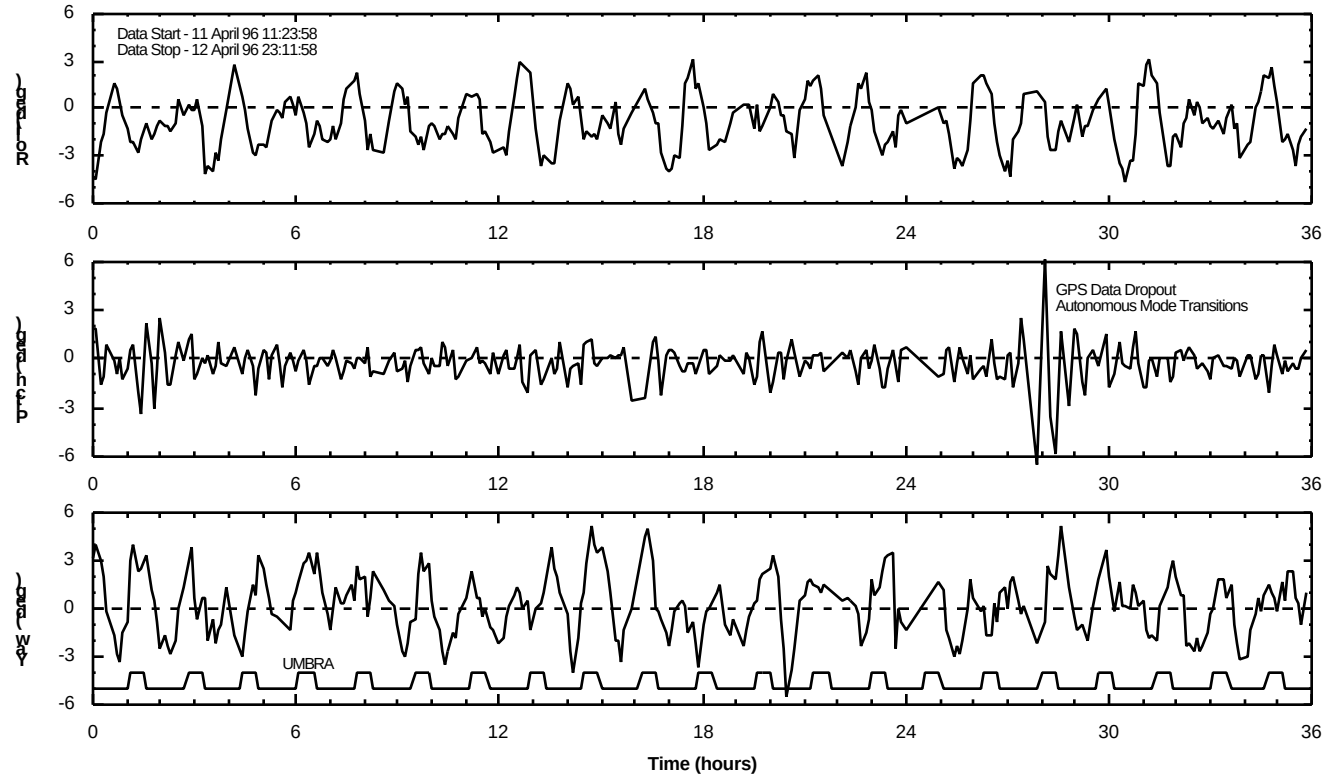

Fig. 10. GPS TANS-B attitude solutions : Long term normal mode performance.

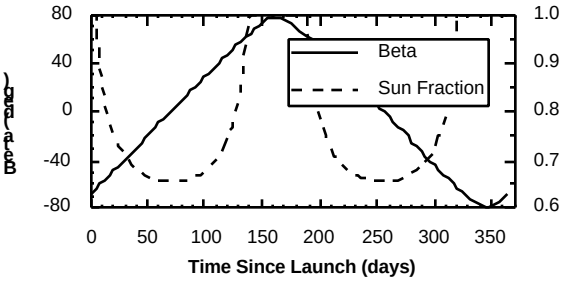

Fig. 11. Orbital solar beta angle and sunlight fraction.

GPS Attitude Solution Noise

The instantaneous error in GPS attitude was estimated from data collected on April 4, 1996 at a 1 Hz rate, significantly faster than the spacecraft's 280 sec nutation period. A linear approximation of the attitude was constructed from the GPS data over 20 sec time intervals. The difference was calculated between each datum and its corresponding linear estimate. The three on-axis errors were combined into a single RMS error. The resulting measurement error is graphed in Fig. 15.

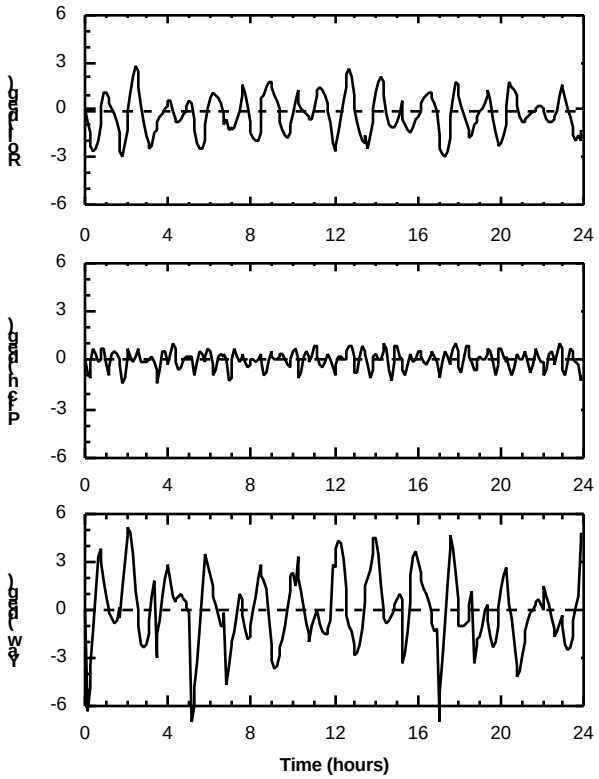

Fig. 12. Simulation of gravity gradient boom thermal snap transient at umbra transition.

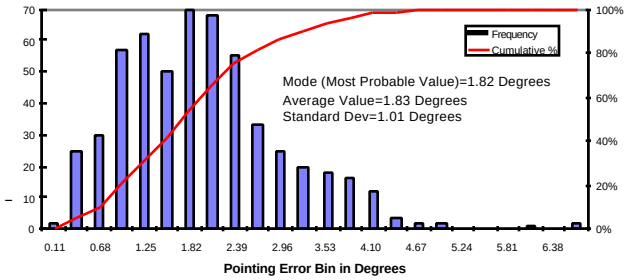

Fig. 13. Normal mode nadir pointing histogram.

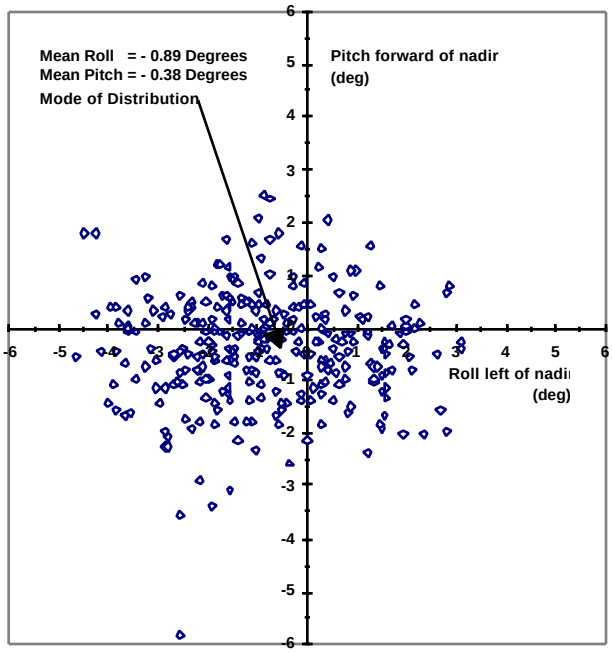

Fig. 14. Normal mode nadir pointing angle distribution.

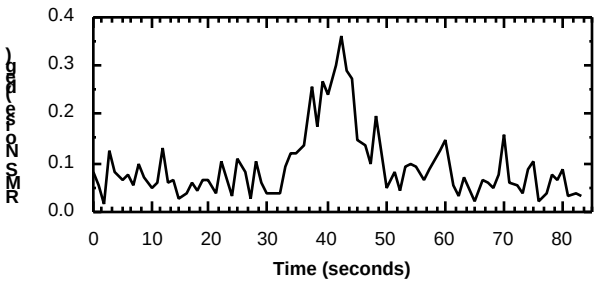

Fig. 15. Instantaneous GPS attitude solution RMS measurement error.

The mean RMS error was 0.09°. This suggests that short term errors in GPS attitude solutions for this sample are usually less than 0.1°, better than had been predicted. The maximum RMS error was 0.36° visible in the middle of the graph. This resulted from a discontinuity in the attitude solution. This shift may be due to a change in satellites being tracked by the GPS receiver. Because this error estimation technique cannot calculate offset errors, this discontinuity suggests that significant offset errors may exist in addition to the instantaneous errors. It is not possible to conclude the magnitude of offset errors.

GPS Attitude Solution Dropout Statistics

GPS data dropouts result from: 1) insufficient satellites, 2) low signal to noise ratios, 3) integer ambiguities, 4) large measurement residuals, or 5) high position dilution of precision. Dropout statistics have been collected from all ACS telemetry files downlinked during the first five months. Each file was scanned for dropouts as indicated by the state of the GPS valid data flag. The start and stop times of each dropout was recorded together with its duration and latitude. A total of 402 dropouts were observed. The sparse nature of telemetry collection suggests a much greater number. An estimate of the frequency of data dropouts was determined by examining the 36 hours of contiguous data from April 11, 1996. The data indicates 33 dropouts. This equates to an average of 1.6 dropouts per orbit.

Dropout duration statistics are presented in Fig. 16. To properly interpret the results it is important to consider the rate at which ACS telemetry was collected. The majority of the data was collected at a rate of 1 sample every 6 minutes. Due to this coarse resolution, the peak in the histogram at 6 minutes implies that the majority of the outages were less than 1 telemetry interval. Collecting data at rates as high as 1 sample every 5 seconds suggests that the majority of dropouts lasted for a single 5 sec ACS cycle, most likely a single attitude frame solution (1 sec).

Table VI lists the distribution of dropouts with spacecraft latitude. There is no apparent correlation between the dropouts and satellite orbital position.

Table VI. Distribution of GPS Attitude Solution Dropouts with Latitude

Latitude Range	Frequency
-90° to -60°	96
-60° to -30°	57
-30° to 0°	59
0° to 30°	75
30° to 60°	51
60° to 90°	64

IV. Conclusions and Future Work

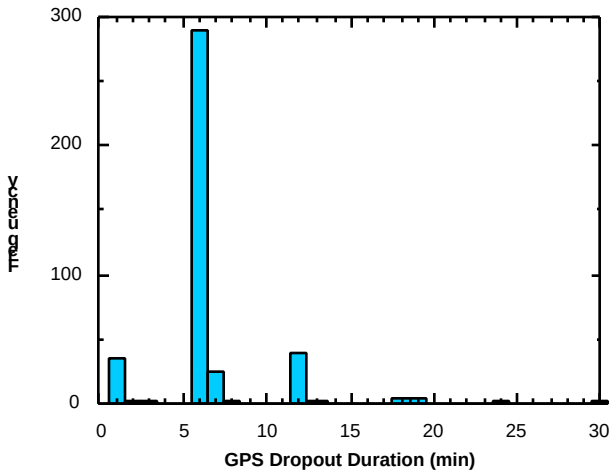

Fig. 16. Distribution of GPS attitude solution dropouts with duration.

REX II has successfully demonstrated for the first time the capability to use real-time GPS attitude knowledge for closed-loop control on-orbit. Evaluation of flight data indicates that overall ACS performance is better than 2.5°, well within spec and that autonomous mode switching provides adequate protection against GPS dropouts. The data suggest that further improvements in performance can be gained by eliminating the passive gravity gradient boom which is the predominate disturbance resulting from thermal snap at umbra transitions. Simulation results have shown that without the boom, performance is improved to better than 2°. Elimination of the boom has the additional advantage of removing the primary source of GPS multipath noise.

Without a precision attitude reference it is difficult to separate GPS performance from that of the controller. The data suggest however, that its performance is better than that predicted by multipath noise models in the range 1°-1.5°, and is more likely in the 0.3°-0.5° range.[4] Additional analysis is being performed to derive an independent measure of spacecraft attitude from the TAM data.[5] The results will further quantify the accuracy of the GPS attitude solution on REX II. The SSTI Clark spacecraft will fly a precision star tracker based attitude reference against which the GPS attitude solution will be compared.

Continued improvements in GPS attitude determination are required to increase accuracy and simplify operations. These include:

- Eliminate the need for pre-launch self survey by incorporating line bias estimation into the receiver firmware.
- Simplify mission operations by eliminating the need to load almanac and/or initial reference position commands at power turn on.
- Reduce the number of attitude solution dropouts.
- Optimize satellite selection algorithms for use in space.

Acknowledgments

The authors wish to express our appreciation to Glen Lighstsey of NASA GSFC, Dr. Penina Axelrad of the University of Colorado and Dr. Lisa Ward of Stanford University for their contributions to the success of GPS attitude determination on REX II.

References

[1] Lightsey E. G., Cohen C. E., Parkinson B. W., "Application of GPS Attitude Determination to Gravity Gradient Stabilized Spacecraft," AIAA GNC Conference, Monterey CA, August 1993.

[2] Cohen C. E., et al., "Space Flight Tests of Attitude Determination Using GPS: Preliminary Results," ION GPS-93 Salt Lake City UT, September 1993.

[3] Ward L. M., Axelrad P., "Spacecraft Attitude Estimation Using GPS: Methodology and Results for RADCAL," ION National Technical Meeting, Anaheim CA, January 1995.

[4] Axelrad P., Ward L. M., "GPS Attitude Determination Performance for REX II," CTASS-S513-002 Final Report, April 1995.

[5] Lightsey E. G., et al., "Flight Results of GPS Based Attitude Determination on the REX II Spacecraft," ION GPS-96, Kansas City MO, September 1996.